Proceedings of the 21st ICSMGE, Vienna, Austria, 14 – 19 June 2026. Pistrol, Adam & Schweiger (eds.)
Published by: ÖGG, Austrian Society for Geomechanics, Salzburg, Austria, ISBN 978-3-9503898-4-5
https://doi.org/10.53243/ICSMGE2026-2115

Analysis of a Thermo-Active Pile Embedded in a Clay Layer Under an Earthquake Excitation

Mehmet Göktuğ İNAYET
Department of Civil Engineering, İstanbul Medeniyet University, Turkey, mgoktug.inayet@medeniyet.edu.tr

Volkan İŞBUĞA
Department of Civil Engineering, İzmir Institute of Technology, Turkey, volkanisbuga@iyte.edu.tr

ABSTRACT: Thermo-active piles are deep foundation systems that support structural loads while simultaneously supplying thermal energy from the ground for heating and cooling systems in buildings. The heat exchange process induces temperature variations along both the pile and the surrounding soil. Such temperature variations may influence the mechanical response of the surrounding soil by altering its shear strength and stiffness. Studies have revealed that clays are more sensitive to temperature variations in terms of strength and stiffness, especially within the typical operating temperature range of thermo-active piles. This study investigates the seismic response of a thermo-active pile embedded in a clay soil, considering temperature-dependent elasticity modulus and cohesion. A three-dimensional finite element model was created to represent the thermo-mechanical response of an energy pile under a steady-state temperature variation. The response of the thermo-active piles was then evaluated under the 2020 Izmir Earthquake excitation and compared to that of identical regular piles. The results are provided to demonstrate the influence of temperature variations on the response of a thermo-active pile embedded in clay soils under seismic excitation and to compare it with the response of a regular pile.

KEYWORDS: Thermo-active piles, energy piles, earthquake response, finite element analysis.

1 INTRODUCTION

Thermo-active piles are innovative deep foundation systems that support the loads acting from the superstructure while simultaneously supplying thermal energy from the ground for heating and cooling systems in buildings. Based on their ability to harness shallow geothermal energy, they are considered renewable energy resources and are often referred to as energy piles. Although thermo-active piles have significant benefits compared to their conventional counterparts, including cost savings (Brandl, 2006; Laloui et al., 2006; Coşman and Kıncay, 2024), energy efficiency (Brandl, 2006; Laloui et al., 2006), and low carbon footprint (Laloui et al., 2006; Amis and Loveridge, 2014), their performance under various loading conditions is an active research area. Main concern for the use of thermo-active piles is that the heat-exchanging process induces temperature variations along the pile and the surrounding soil, which in turn produces additional stress and strains, and influences the load transfer behavior of the pile (Bourne-Webb et al., 2009; Amatya et al., 2012). Moreover, temperature variations may influence the strength and stiffness of the surrounding soil (Laguros, 1969; Murayama, 1969; Abuel-Naga et al., 2007; Cekerevac and Laloui, 2010). Studies have revealed that clays are more sensitive to temperature variations than sands within the typical operating temperature range of thermo-active piles (Di Donna et al., 2016; Yavari et al., 2016; Maghsoodi et al., 2020).

Laguros (1969) conducted unconfined compression tests on clays under the influence of temperature and found that the increase in temperature increased the unconfined compression strength of the clay. Abuel-Naga et al. (2007) investigated the temperature effect on the shear strength and yielding behavior of soft Bangkok clay and found that the strength and stiffness of the clay increased with increasing temperatures. Cekerevac and Laloui (2010) studied the influence of temperature on the behavior of Kaolin clay under cyclic shear loading and found that the heating improved the soil's resistance through thermal hardening. They suggested that the heating may have a positive effect on the earthquake response of clays. Murayama (1969) investigated the effect of temperature on the elastic modulus of Osaka clay and found that the elastic modulus reduces with increasing temperature. There are several works incorporating variations in elasticity modulus and undrained cohesion due to heating operations of thermo-active piles (Garakani et al., 2022; Heidari et al., 2022, 2024; Ding et al., 2024). Many researchers worked on the behavior of thermo-active piles under static loading conditions (Laloui et al., 2006; Bourne-Webb et al., 2009; Amatya et al., 2012; Olgun et al., 2014, 2015; Ng et al., 2014; Saggu and Chakraborty, 2015; Khosravi et al., 2016; McCartney and Murphy, 2017; Arzanfudi et al., 2020; Garakani et al., 2022; Heidari et al., 2022, 2024; Zhao et al., 2023; Peng et al., 2023; Ding et al., 2024; Song et al., 2025; Erginag et al., 2025). However, the response of thermo-active piles to earthquake excitation has received considerably less attention. Moreover, the earthquake response of piles is inherently more complex, involving kinematic pile-soil interaction from the movement of the surrounding soil and the inertial effects from the interaction between the pile and the superstructure (Finn, 2005), and therefore requires dedicated investigation. Uncertainties in this area may lead to insufficient design of such foundation types in earthquake-prone regions. To the authors' knowledge, only one recent study by Kontoni and Farghaly (2024) has examined the seismic response of thermo-active piles. They investigated the effect of heating-cooling cycles on the seismic response of a high-rise building with a piled raft foundation under several earthquake motions, and found that the heating phase of the thermo-active pile may increase the lateral displacements, while the cooling phase may increase the base shear force. However, further research is needed to address a wider range of conditions, including the soil's behaviour to temperature variations.

This study focuses on the relative difference in response between a thermo-active single pile and an identical regular pile embedded in a clay under the 2020 Izmir Earthquake excitation, accounting for temperature-dependent undrained cohesion and Young's modulus of the clay. The analyses were performed considering two pile length-to-diameter ratios of 30 and 40, with a constant diameter of 0.5 m. For the specific cases considered in this study, the findings offer preliminary insight into the potential applicability of thermo-active piles in earthquake-prone regions where soils exhibit temperature sensitivity within the typical operational range.

2 NUMERICAL MODELING

A 3D finite element model is constructed in Abaqus to evaluate the earthquake response of vertically loaded thermo-active

piles. The geometry and imposed boundary conditions of the finite element model are shown in Figure 1 and Figure 2.

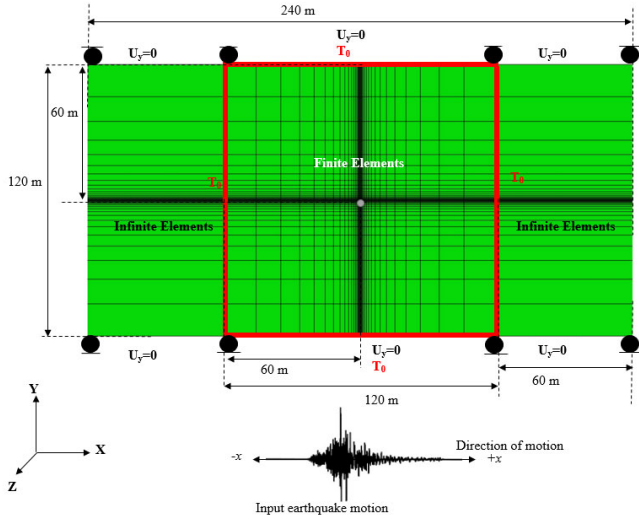

Figure 1. Top view of the model geometry and boundary conditions

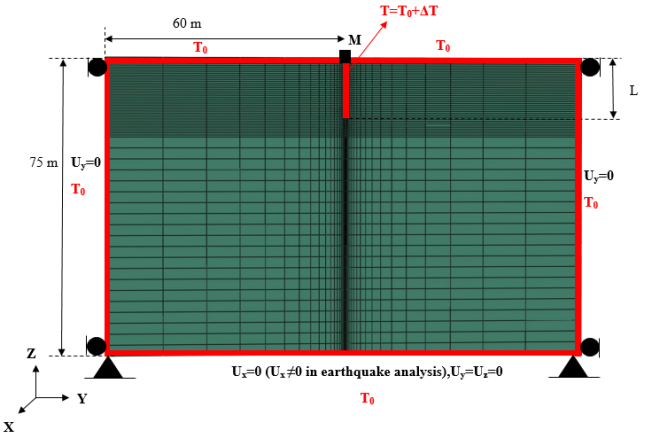

Figure 2. Side view of the model geometry and boundary conditions

The pile is placed at the center of the model. Two different pile length-to-diameter ratios, L/D=30 and L/D=40, are investigated in the analyses. For both L/D ratios, the pile diameter was 0.5 m, and the pile length was changed accordingly. Dimensions of the finite element domain are 75 m in depth and 120 m in both length and width, which is large enough to avoid boundary effects in static analysis. Infinite elements are employed to represent the far-field region by extending the boundaries in the direction of motion. These elements provide a quiet boundary by introducing boundary damping constants, thereby minimizing the reflection of the outgoing waves at the boundaries (Abaqus User's Manual, 2012). Displacement boundary conditions were applied to prevent rigid-body movement. Displacements on the base of the soil domain were constrained in the x, y, and z-directions in the static and thermo-mechanical analyses. During the dynamic analysis, the earthquake motion was introduced to the base of the model in the x-direction. Therefore, the base of the model was allowed to displace in the direction of motion.

The length of the infinite elements was selected based on the guidelines provided in the Abaqus User's Manual (2012), which recommends locating the outer nodes of the infinite elements at a radial distance equal to twice the distance between the finite element boundary and a reference point referred to as the pole. The pole is typically defined as the point of load application. Herein, the center of the pile serves as the pole, and the length of the infinite element was chosen as half the length of the finite element domain, as illustrated in Figure 3.

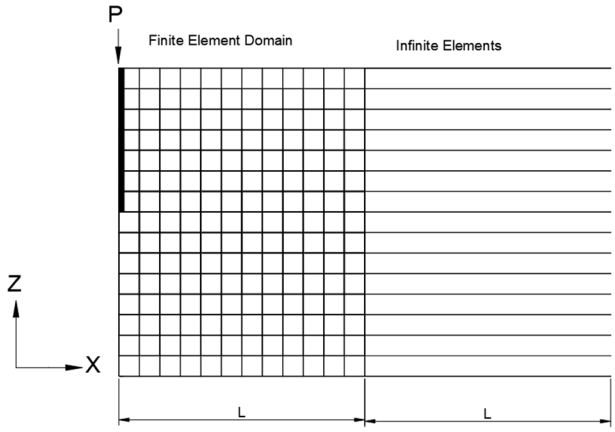

Figure 3. Infinite element size requirement (Abaqus User's Manual, 2012)

A point mass element is placed at the center of the pile head to simulate the structure's weight. In this study, the mass was 51 tons, which subjects the pile to a vertical load of 500 kN. Kinematic coupling was applied between the point mass and the pile head nodes to ensure that they experience the same displacement under vertical load.

The initial temperatures of the soil domain and the pile were both set to 15 °C. Constant temperature boundary conditions (T=15 °C) were defined on the ground surface, side boundaries, the intersecting nodes between the finite elements and infinite elements, and the base of the model. At the heating step, the pile temperature is increased to 36 °C. The temperature value was selected within the typical operating temperature range of thermo-active piles (De Moel et al., 2010; Ng et al., 2014). It was assumed that the system reaches thermal equilibrium at the end of the heating analysis.

Finite element modeling of thermo-active piles requires multiple steps to simulate the sequence of loading conditions, starting from the initial geostatic conditions, followed by the application of mechanical loads, thermal loading, and lastly the earthquake motion. The steps were defined in order as follows:

1. Initial step: The geostatic stress and temperature are defined in this step as the initial conditions, and the displacement boundary conditions are introduced to the model.
2. Geostatic step: The gravity loading is applied to both the pile and the soil domain to bring the model to geostatic equilibrium, without applying gravity load to the point mass.
3. Static step: Applying gravity loading to the point mass, which simulates an axial load of 500 kN at the pile head.
4. Steady-state coupled temperature-displacement step: Increasing the pile temperature to 36 °C, and obtaining a temperature field based on the steady-state heating conditions.
5. Dynamic step: Applying the 2020 Izmir earthquake motion to the base of the finite element domain using an implicit integration scheme.

The heating step was excluded for the regular pile, and the remaining steps were the same. For the entire analysis, the pile-soil interface was assumed to be perfectly bonded for both piles.

An 8-node trilinear displacement and temperature element formulation (C3D8T) was used for pile and soil, and an 8-node linear, one-way infinite (CIN3D8) was used for the infinite domain. The point mass was introduced as a mass element.

Mesh is refined near the pile in order to increase the accuracy of the solution. Mesh sensitivity studies were carried out, and 83,040 elements were deemed sufficient to balance the accuracy of the solution and the computational cost.

Table 1 demonstrates the material properties used in this study.

Table 1. Material properties.

Parameter	Clay	Pile
Density, ρ (kg/m^3)	1840	2500
Young's modulus, E_0 (MPa)	25	27,380
Poisson's ratio, v	0.495	0.2
Cohesion, c (kPa)	50	-
Friction angle, ϕ (°)	1	-
Coefficient of thermal expansion, α_s (1/°C)	5x10^{-6}	10^{-5}
Thermal conductivity, λ (W/m °C)	1.5	2.1
Specific heat capacity, c_s (J/kg °C)	1500	800

The pile was modeled as a linear elastic material. The mechanical and thermal properties of the pile were taken from Saggu and Chakraborty (2015). Soil properties were modeled using the Mohr-Coulomb material model. Thermal properties of the clay were taken from Arzanfudi et al. (2020), while the mechanical properties were chosen by considering typical undrained clay properties. Clay with an undrained shear strength of 50 kPa is within the range for a medium-stiff clay (Das and Sobhan, 2014). While the clay is in undrained conditions, a small friction angle is assigned to avoid convergence problems. Young's modulus of the clay was selected as $500s_u$, which is within the range that relates the Young's modulus to the undrained shear strength of clay (Bowles and Guo, 1996). It was assumed that the undrained cohesion and Young's modulus of clay do not change with depth, and the selected values represent the overall site soil properties. Temperature-dependent undrained cohesion and soil Young's modulus were employed based on the formulations provided by Heidari et al. (2022), who developed these formulations from the findings of Laguros (1969) and Murayama (1969) as follows:

$$c_{u(T)} = c_{u,0} + 0.53\Delta T \quad (1)$$

$$E_{s(T)} = E_{s,0} - 0.39\Delta T \quad (2)$$

where $c_{u(T)}$ is the temperature-dependent undrained cohesion (kPa), $c_{u,0}$ is the initial undrained cohesion (kPa), $E_{s(T)}$ is the temperature-dependent soil Young's modulus (MPa), $E_{s,0}$ is the initial soil Young's modulus (MPa), and ΔT is the temperature change (°C).

Although Mohr-Coulomb model has distinct limitations in seismic analyses such as its inability to capture soil nonlinearity and inherent material damping at small strains (Soleimanian et al., 2023), it was deemed appropriate for this preliminary study which aims to capture the differences in the earthquake response of an energy pile and the identical regular pile under the influence of temperature-dependent soil shear strength and Young's modulus.

In the analyses, the 2020 Izmir Earthquake motion was used as the input motion. The acceleration history of the 2020 Izmir Earthquake was taken from the TK3519 station in the AFAD database (Disaster and Emergency Management Authority, 2023). The acceleration histories were pre-processed using a 2nd-order band-pass Butterworth filter to eliminate low- and high-frequency noise. The recording station site was classified as ZE (Kömeç Mutlu et al., 2023), which corresponds to loose sand and gravel or soft to stiff clay, according to the Turkish Building Earthquake Code (2018). Since the motion was recorded at the surface, which is already influenced by local site effects, 1D deconvolution analyses were carried out using DEEPSOIL in order to convert the surface motion into the bedrock motion. These analyses were carried out in the frequency domain under the assumption of linear elastic soil conditions. Input soil properties were derived from the properties of the clay used in the present study, which were consistent with the ZE site classification. A rigid bedrock boundary was assumed at the base of the model. After obtaining the bedrock motion through deconvolution, baseline correction was applied to remove residual drift. After processing the N-S and E-W components of the motion, it was observed that the N-S component exhibits higher peak ground acceleration (PGA), Arias intensity, and cumulative absolute velocity (CAV) than the E-W component. These parameters are commonly included among the intensity measures that are used to describe the destructiveness of ground motions (Sharma et al., 2025). The PGA values were 0.1g and 0.08g, the Arias intensities were 0.5 m/s and 0.4 m/s, and the CAV values were 0.56 g.s and 0.53 g.s for the N–S and E–W components, respectively. Therefore, the N-S component of the motion was adopted in this study. The input motion is illustrated in Figure 4.

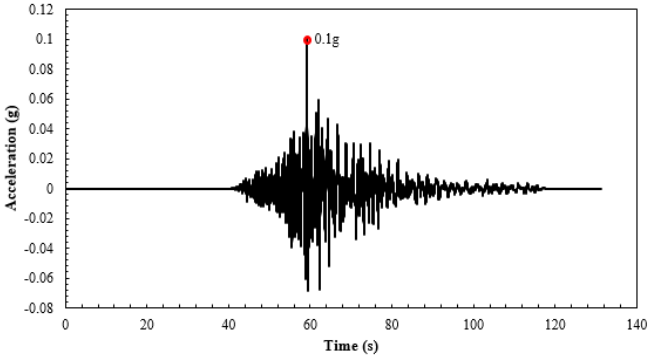

Figure 4. 2020 Izmir Earthquake motion

Damping of the pile and soil was included using a two-mode Rayleigh damping scheme from the following equation (Hudson et al., 1994):

$$\alpha = 2\xi \frac{\omega_1 \omega_2}{\omega_1 + \omega_2} \quad (3)$$

$$\beta = \frac{2\xi}{\omega_1 + \omega_2} \quad (4)$$

where ξ is the target damping ratio (%), α is the mass-proportional Rayleigh damping coefficient, β is the stiffness-proportional Rayleigh damping coefficient, ω_1 is the first target mode (rad/s), and ω_2 is the second target mode (rad/s).

In this study, 5% target damping ratio was adopted. The first target mode (ω_1) was set to the natural frequency of the overall system, and the second target mode (ω_2) was taken as the predominant frequency of the input motion (Hashash et al., 2010). According to Hudson et al. (1994), ω_2 should be adjusted as follows:

- Compute the ratio of ω_2/ω_1.
- Round this ratio to the nearest odd integer greater than ω_2/ω_1.
- Multiply the odd integer by ω_1 to obtain adjusted ω_2.

This procedure helps prevent over-damping within the predominant frequency range of the input motion.

A modal analysis was conducted to determine the natural frequency of the overall system, and it was computed as 0.2 Hz. The predominant frequency of the 2020 Izmir Earthquake motion was identified as 1 Hz from the FFT. By following the

procedure outlined by Hudson et al. (1994), and converting the target modes into circular frequencies for substitution into Equations (3) and (4), the Rayleigh damping coefficients α and β were calculated as 0.1047 and 0.01326, respectively.

3 RESULTS

Figure 5 and Figure 6 present the steady-state temperature field obtained at the end of the heating phase.

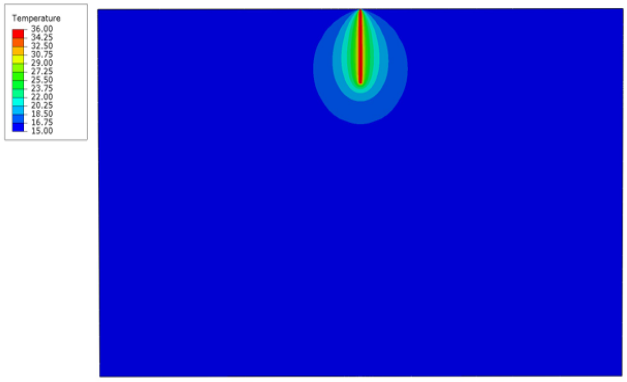

Figure 5. Temperature distribution at the end of heating for L/D=30

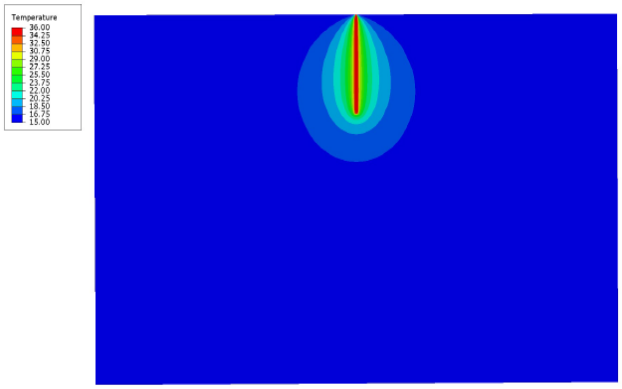

Figure 6. Temperature distribution at the end of heating for L/D=40

Figure 5 and Figure 6 show the temperature distribution across the entire model for L/D=30 and L/D=40, respectively, highlighting the zone affected by temperature changes during the heating phase and thus the extent of thermal effects.

Figure 7 illustrates the normalized vertical displacement distribution along the normalized pile depth at the end of the static loading and heating steps.

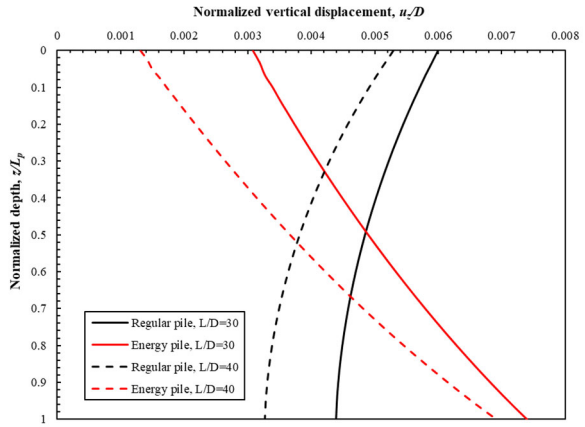

Figure 7. Normalized vertical displacements along the piles at the end of static and heating steps

From Figure 7, it can be seen that at the end of the heating phase, the pile experiences elongation due to thermal expansion, with upward movement above the null-point and downward movement below it. The null-point, defined as the point of zero thermal vertical displacement, is located at approximately mid-depth of the pile for both L/D=30 and L/D=40. Null-point can be seen where the vertical displacements of the static step and the heating step coincide. Longer pile experienced greater elongation. Such elongation behavior aligns with typical observations from a pile's response to heating (Bourne-Webb et al., 2009; Amatya et al., 2012; Khosravi et al., 2016). We obtained the same response while explicitly incorporating temperature-dependent variations in soil elastic modulus and undrained cohesion. Therefore, this finding reveals that the entire heating operation, including modulus and undrained cohesion variations in the surrounding soil, altered the response of the pile under the static loading condition, with the elongation pattern remaining consistent with that reported in previous studies.

Figure 8 and Figure 9 present a comparison of the acceleration responses taken from the pile head for the thermo-active pile and its identical regular counterpart with L/D=30 and L/D=40, respectively.

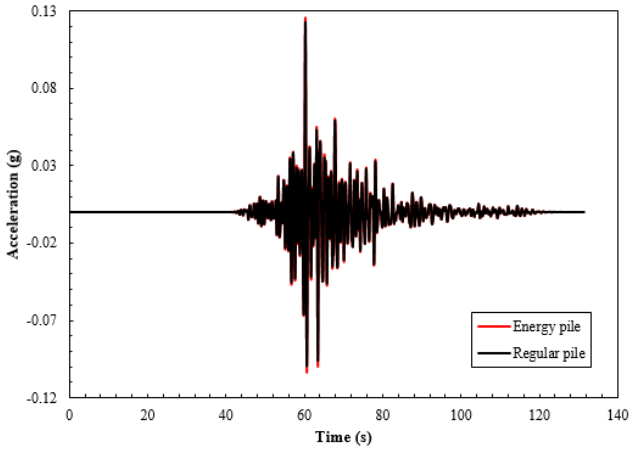

Figure 8. Acceleration response at the pile head for L/D=30

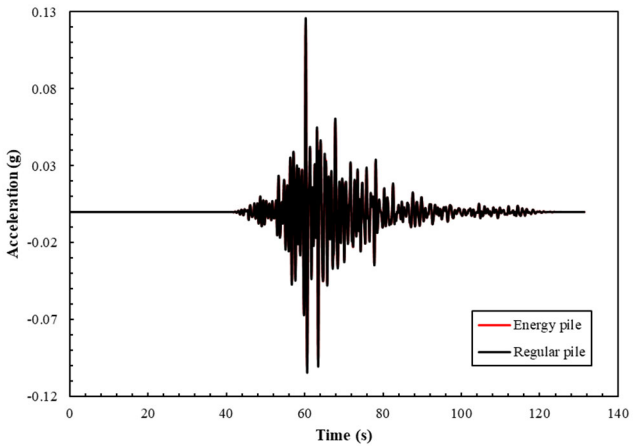

Figure 9. Acceleration response at the pile head for L/D=40

As shown in Figure 8, the thermo-active pile with L/D=30 reached a peak acceleration of 0.126g at the pile head, whereas its identical regular counterpart reached 0.123g. From Figure 9, it can be seen that the peak acceleration of the pile with L/D=40 is identical to the L/D=30 case. The relative difference in peak accelerations between the thermo-active and regular piles was found to be approximately 2.24% for both cases, which is quite

small. Therefore, the influence of heating on the pile's acceleration response was minimal for the considered cases.

Figure 10 and Figure 11 illustrate the lateral displacement response at the pile head for both the thermo-active and regular piles with *L/D*=30 and *L/D*=40, respectively.

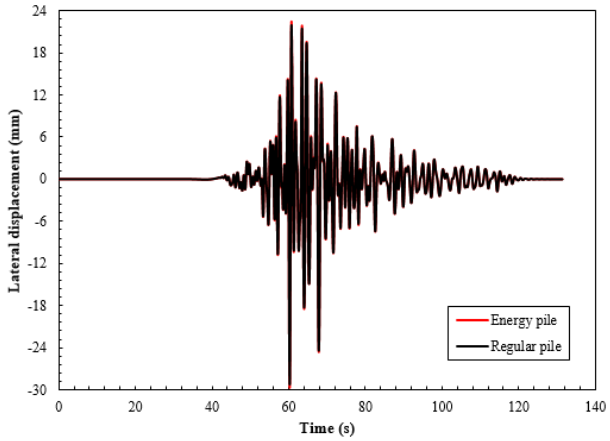

Figure 10. Lateral displacements at the pile head for *L/D*=30

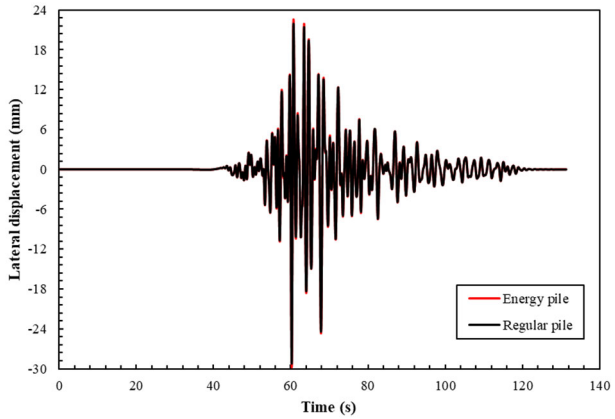

Figure 11. Lateral displacements at the pile head for *L/D*=40

As can be seen in Figure 10, the lateral displacement of the thermo-active pile with *L/D*=30 exhibited no significant deviation from that of its identical regular counterpart. The peak lateral displacement was 29.7 mm for the thermo-active pile and 29.2 mm for the regular pile. This represents a 1.7% relative difference in peak lateral displacement between the thermo-active and regular piles. This change is practically negligible. From Figure 11, it can be seen that the lateral displacement of the pile with *L/D*=40 is nearly identical to the *L/D*=30 case. For *L/D*=40, the peak lateral displacement was 29.8 mm for the thermo-active pile and 29.2 mm for the identical regular pile. The relative difference in peak lateral displacements between the thermo-active and regular piles was approximately 2% for *L/D*=40 case, which is insignificant in practice. Therefore, it can be concluded that the changes in lateral pile head displacement due to the heating operation are negligible.

Figure 12 presents the normalized lateral displacement variations with *L/D* ratio.

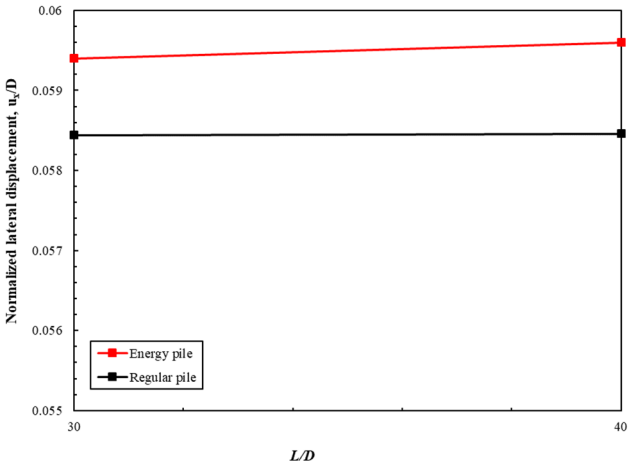

Figure 12. Normalized lateral pile head displacement with *L/D*

As can be seen in Figure 12, the normalized lateral pile head displacements are nearly identical for *L/D*=30 to *L/D*=40 cases. Slight increases in normalized lateral pile head displacement were observed for the thermo-active piles. However, these changes were minor.

Overall, it was observed that the changes in the earthquake response of the pile due to heating are practically negligible and do not significantly alter the performance of the pile.

4 CONCLUSIONS

In this study, the response of a thermo-active pile embedded in clay under the 2020 Izmir Earthquake excitation was investigated, incorporating temperature-dependent undrained shear strength and Young's modulus of the soil, and compared to that of an identical regular pile. Pile length-to-diameter ratios of 30 and 40 were considered in this study, having a constant diameter of 0.5 m. The findings present a preliminary insight into the potential use of thermo-active piles in earthquake-prone regions where the soil properties are sensitive to temperature variations. The entire heating operation, including temperature-dependent variations in modulus and undrained shear strength variations in the surrounding soil, altered the pile's response under static vertical load, with a typical elongation behavior observed in practice. However, the heating operation did not noticeably alter the performance of the piles under earthquake loading, even with the temperature-induced reductions in stiffness of the surrounding soil. Moreover, only minor differences were observed in its acceleration and lateral displacement response to earthquake motion. While the results are promising for the use of thermo-active piles in earthquake-prone regions, the scope of this study was limited to two specific cases. Therefore, further analysis is required to deepen our understanding by considering a wider range of pile length-to-diameter ratios, ground motions and temperature amplitudes. Overall, these findings provide a basis for more comprehensive future investigations.

5 REFERENCES

ABAQUS 2012. Analysis User's Manual, Version 6.14. Dassault Systèmes Simulia, Inc.

Abuel-Naga, H. M., Bergado, D. T., Lim, B. F. 2007. Effect of temperature on shear strength and yielding behavior of soft Bangkok clay. *Soils and Foundations*, 47(3), 423–436.

Amatya, B. L., Soga, K., Bourne-Webb, P. J., Amis, T., Laloui, L. 2012. Thermo mechanical behaviour of energy piles. *Géotechnique*, 62(6), 503–519.

Amis, T., Loveridge, F. 2014. Energy piles and other thermal foundations, developments in UK practice and research. *REHVA Journal*, 51(1), 32-35.

Arzanfudi, M. M., Al-Khoury, R., Sluys, L. J., Schreppers, G. M. A. 2020. A thermo-hydro-mechanical model for energy piles under cyclic thermal loading. *Computers and Geotechics*, 125, 1-18.

Bourne-Webb, P. J., Amatya, B., Soga, K., Amis, T., Davidson, C., Payne, P. 2009. Energy pile test at Lambeth College, London: geotechnical and thermodynamic aspects of pile response to heat cycles. *Geotechnique*, 59(3), 237–248

Bowles, J. E., and Guo, Y. 1996. *Foundation analysis and design*. 5th edition. New York: McGraw-hill.

Brandl, H. 2006. Energy foundations and other thermo-active ground structures", *Geotechnique*, 56(2), 81–122

Cekerevac, C., Laloui, L. 2010. Experimental analysis of the cyclic behaviour of kaolin at high temperature. *Géotechnique*, 60(8), 651–655.

Coşman, S., and Kıncay, O. 2024. Investigation of an energy pile appli cation and its economic analysis. *European Mechanical Science*, 8(1), 1–10.

Das, B. M., and Sobhan, K. 2014. *Principles of Geotechnical Engineering*. 8th edition. Boston: Cengage Learning.

De Moel, M., Bach, P. M., Bouazza, A., Singh, R. M., and Sun, J. O. 2010. Technological advances and applications of geothermal energy pile foundations and their feasibility in Australia. *Renewable and Sustainable Energy Reviews*, 14(9), 2683-2696.

Di Donna, A., Ferrari, A., and Laloui, L. 2016. Experimental investigations of the soil–concrete interface: physical mechanisms, cyclic mobilization, and behaviour at different temperatures. *Canadian Geotechnical Journal*, 53(4), 659-672.

Ding, X., Zhang, D., Wang, C., Bouazza, A., and Kong, G. 2024. Thermally induced mechanical interactions of energy pile groups subjected to cyclic nonsymmetrical thermal loading. *Computers and Geotechnics*, 167, 106053.

Disaster and Emergency Management Authority (AFAD). 2018. *Turkish Building Earthquake Code, 2018*. Ankara: The Presidency of Republic of Turkey.

Disaster and Emergency Management Authority (AFAD). 2023. *Turkish National Strong Motion Network (TADAS)*. [Online] Available at: https://tadas.afad.gov.tr/ [Accessed 11th August 2023].

Erginag, U. C., Guner, M., Polat, S., Sutman, M., and Cinicioglu, O. 2025. Thermally Induced Tensile Hoop Stresses in Energy Piles: Implications for Design and Operation. *Geomechanics for Energy and the Environment*, 100702.

Finn, L. W. D. 2005. A study of piles during earthquakes: issues of design and analysis. *Bulletin of Earthquake Engineering*, 3(2), 141-234.

Garakani, A. A., Heidari, B., Jozani, S. M., and Ghasemi-Fare, O. 2022. Numerical and analytical study on axial ultimate bearing capac ity of fixed-head energy piles in different soils. *International Journal of Geomechanics*, 22(1), 04021258

Hashash, Y. M., Phillips, C., Groholski. D. R. 2010. Recent Advances in Non-Linear Site Response Analysis. 5th International Conference on Recent Advances in Geotechnical Earthquake Engineering and Soil Dynamics, San Diego, California.

Heidari, B., Garakani, A. A., Jozani, S. M., and Tari, P. H. 2022. Energy piles under lateral loading: Analytical and numerical investigations. *Renewable Energy*, 182, 172-191.

Heidari, B., Yoosefi, S., and Garakani, A. A. 2024. Assessing the effects of horizontal loads on the ultimate vertical bearing capacity of energy piles: A comparative numerical and analytical study. *Renewable Energy*, 234, 121204.

Hudson, M., Idriss, I. M., and Beikae, M. 1994. QUAD4M—A computer program to evaluate the seismic response of soil structures using finite element procedures and incorporating a compliant base. Center for Geotechnical Modeling, Deptartment of Civil and Environmental Engineering, University of California, Davis, California.

Khosravi, A., Moradshahi, A., McCartney, J., and Kabiri, M. 2016. Numerical analysis of energy piles under different boundary conditions and thermal loading cycles. In E3S Web of Conferences, 9, 05005.

Kontoni, D. P. N., Farghaly, A. A. 2024. Investigation of the effect of energy piles on the seismic response of RC high-rise building with piled raft foundation. *Coupled Systems Mechanics*, 13(5), 433-457.

Kömeç Mutlu, A., Mert Tuğsal, Ü., and Cambaz, M. 2023. Zemin Hâkim Frekanslarının Farklı Algoritmalarla Belirlenmesi: İzmir Örneği. *Doğal Afetler ve Çevre Dergisi*, 9(1), 58-70.

Laguros, J. G. 1969. Effect of temperature on some engineering properties of clay soils. Highway research board special report (103), Conference on effects of temperature and heat on engineering behaviour of soils, Sponsored by The Committee on Physico-Chemical Phenomena in Soils, 186-193.

Laloui L, Nuth M, Vulliet L. 2006. Experimental and numerical investigations of the behaviour of a heat exchanger pile. *International Journal for Numerical and Analytical Methods in Geomechanics*, 30, 763–781.

Maghsoodi, S., Cuisinier, O., and Masrouri, F. 2020. Thermal effects on mechanical behaviour of soil–structure interface. *Canadian Geotechnical Journal*, 57(1), 32-47.

McCartney, J. S., and Murphy, K. D. 2017. Investigation of potential dragdown/uplift effects on energy piles. *Geomechanics for Energy and the Environment*, 10, 21-28.

Murayama, S. 1969. Effect of temperature on elasticity of clays. Highway Research Board Special Report (103), Conference on effects of temperature and heat on engineering behaviour of soils, Sponsored by The Committee on Physico Chemical Phenomena in Soils, 194-203.

Ng, C. W. W., Shi, C., Gunawan, A., and Laloui, L. 2014. Centrifuge modelling of energy piles subjected to heating and cooling cycles in clay. *Geotechnique letters*, 4(4), 310-316.

Olgun, C. G., Ozudogru, T. Y., Abdelaziz, S. L., and Senol, A. 2015. Long-term performance of heat exchanger piles. *Acta Geotechnica*, 10(5), 553-569.

Olgun, C. G., Ozudogru, T. Y., and Arson, C. F. 2014. Thermo-mechanical radial expansion of heat exchanger piles and possible effects on contact pressures at pile–soil interface. *Géotechnique Letters*, 4(3), 170-178.

Peng, C., Ding, X., Wang, C., Kong, G., and Wu, D. 2023. Thermo-mechanical characteristics of laterally loaded energy piles under multiple heating-cooling cycles in mountain area. *Journal of Energy Storage*, 63, 107020.

Saggu, R, Chakraborty, T. 2015. Cyclic Thermo-Mechanical Analysis of Energy Piles in Sand. *Geotechnical and Geololgical Engineering*, 33, 321-342.

Sharma, M., Singh, S., Prasad, P., Anand, V., and Islam, N. 2025. Correlation analysis of ground motion intensity measures for seismic damage assessment: insights from near and far field records. *Asian Journal of Civil Engineering*, 26(5), 1973-2004.

Soleimanian, N., Bazaz, J. B., Akhtarpour, A., and Garivani, S. 2023. Effects of constitutive soil models on the seismic response of an offshore jacket platform in clay by considering pile-soil-structure interaction. *Soil Dynamics and Earthquake Engineering*, 174, 108165.

Song, H., Pereira, J. M., Tang, A. M., and Pei, H. 2025. Thermally-induced long-term behavior of energy piles under inclined load in saturated clay. *Canadian Geotechnical Journal*, 62, 1-23.

Yavari, N., Tang, A. M., Pereira, J.-M., and Hassen, G. 2016. Effect of temperature on the shear strength of soils and the soil–structure interface. *Canadian Geotechnical Journal*, 53(7), 1186–1194.

Zhao, R., Leung, A. K., Knappett, J. A. 2023. Thermally induced ratcheting of a thermo-active reinforced concrete pile in sand under sustained lateral load. *Géotechnique*, 73(9), 826-839.